Relationships between primary productivity and bottom-water oxygenation off northwest Africa during the last deglaciation

JQS

HELENA L. FILIPSSON,[1,2]* OSCAR E. ROMERO,[2,3] JAN-BEREND W. STUUT[2,4] and BARBARA DONNER[2]

[1]Department of Earth and Ecosystem Sciences, Division of Geology, Lund University, Sölveg. 12, SE-223 62 Lund, Sweden
[2]MARUM – Center for Marine Environmental Sciences, University of Bremen, Germany
[3]Instituto Andaluz de Ciencias de la Tierra (UGR-CSIC), Campus Fuentenueva, Facultad de Ciencias, Universidad de Granada, Granada, Spain
[4]NIOZ – Royal Netherlands Institute for Sea Research, Den Burg, the Netherlands

ABSTRACT: The upwelling region off northwest Africa is one of the most productive regions in the world ocean. This study details the response of surface- and deep-water environments off Mauritania, northwest Africa, to the rapid climate events of the last deglaciation, especially the Bølling–Allerød (15.5–13.5 ka BP) and Younger Dryas (13.5–11.5 ka BP). A high accumulation rate gravity core GeoB7926-2, recovered at ~20° N, 18° W, was analysed for the grain size distribution of the terrigenous sediment fraction, the organic carbon content, diatom and benthic foraminifera communities. Humid conditions were observed during the Bølling–Allerød with a high contribution of fluvial sediment input. During the Younger Dryas intensified trade winds caused a larger sediment input of aeolian dust from the Sahara and more intense upwelling with higher primary productivity, as indicated by high diatom concentrations. The abrupt and large increase of organic matter caused low oxygen conditions at the sea floor, reflected by the poor benthic foraminiferal fauna and the dominance of the low-oxygen-tolerant foraminiferal species *Bulimina exilis*. This is surprising since low-oxygen conditions have not been recorded during modern times at the sea floor in this region, despite present-day intensive upwelling and high primary productivity. After the Younger Dryas, more humid conditions returned, diatom abundance decreased and *B. exilis* was replaced by typical deep-sea species as found in the region today, indicating the return of more oxygenated conditions at the sea floor. Copyright © 2011 John Wiley & Sons, Ltd.

KEYWORDS: upwelling; Younger Dryas; benthic foraminifera; low-oxygen; NW Africa.

Introduction

There has been increased interest to better understand how both the land environment in northwest Africa and the surrounding marine areas have responded to short-term climate variations, such as the rapid events related to the last deglaciation and events occurring during the Holocene (deMenocal *et al.*, 2000a,b; Kuhlmann *et al.*, 2004; Kim *et al.*, 2007; McGregor *et al.*, 2007; Mulitza *et al.*, 2008,; Romero *et al.*, 2008). The northwest Africa region is presently marked with extensive coastal upwelling (Mittelstaedt, 1991) and several studies indicate that the intensity of the upwelling has varied considerably during the last deglaciation and during the Holocene (e.g. McGregor *et al.*, 2007; Romero *et al.*, 2008). Several multi-parameter reconstructions, covering the late Quaternary in subtropical northern Africa, illustrate the complex relationship between Saharan ecosystems and climate throughout the periods of aridification (Gasse, 2000; Garcin *et al.*, 2007; Talbot *et al.*, 2007; Kröpelin *et al.*, 2008; Castaneda *et al.*, 2009; Mulitza *et al.*, 2010) as well as abrupt, large-scale changes along the northwest African upwelling system (deMenocal *et al.*, 2000a,b; Kuhlmann *et al.*, 2004; Adkins *et al.*, 2006; Kim *et al.*, 2007). Our understanding of how the marine environments along the northwest African coast responded to rapid climate changes and subsequent changes in upwelling, however, remains incomplete. One reason for this is the scarcity of suitable high-resolution sediment cores, which also contain appropriate proxy variables representing both the land and marine environments.

Present hydrographic and nutrient conditions off Mauritania are highly favourable for diatom occurrence (Romero *et al.*,

2002, and references therein). Diatom productivity depends on the availability of silicate and other nutrients in the upwelled waters, just as the accumulation of opaline debris in sediments depends on the availability of silicate in the waters below the mixed layer (Ragueneau *et al.*, 2000). On an annual basis, the relative contribution of diatoms to primary productivity in the region is variable; Nelson *et al.* (1995) and Tréguer *et al.* (1995) proposed upper limits of 75% in coastal upwelling areas.

Benthic foraminifera have a wide distribution and a high fossilisation potential; two of the most important limiting factors for their distribution are dissolved oxygen concentrations of bottom and pore waters, and the organic matter supply with respect to quantity, quality, and seasonality (e.g. Loubere and Fariduddin, 1999; Murray 2001; Jorissen *et al.*, 2007). Hence by studying the benthic foraminiferal species composition and abundance it is possible not only to reconstruct the benthic environment but also surface productivity changes and organic matter fluxes to the sea floor (e.g. Herguera and Berger, 1991; Loubere, 1991; Thomas *et al.*, 1995).

Here we present a palaeorecord with a submillennial temporal resolution, collected off Cape Blanc, Mauritania; the record's accumulation rate varies between 10 to 340 cm ka^{-1} (Romero *et al.*, 2008). The approach of combining palaeoenvironmental indicators representing terrestrial humidity/aridity variations and wind intensity (through grain size analysis), surface-water productivity (through diatom analysis and benthic foraminifera) and deep-ocean ventilation (by benthic foraminiferal analysis) allows an investigation of past interactions between these three subsystems off northwest Africa. The grain size analyses, interpreted using an end-member modelling approach, and the benthic foraminiferal data are presented here for the first time, whereas the diatom record has been published in detail by Romero *et al.* (2008). The comparison of all these data provides a more detailed

*Correspondence: Helena L. Filipsson, as above.
E-mail: Helena.Filipsson@geol.lu.se

picture of the interactions between the systems and helps to better understand rapid palaeoclimate variations in low-latitude coastal upwelling systems during the last deglaciation.

Study area

Owing to the present-day arid conditions, the area off Cape Blanc is under the major Sahara dust plume that nowadays blows into the Atlantic Ocean (Fig. 1). The Sahara and Sahel regions in northwest Africa are presently arid/semi-arid. However, several studies have shown that environmental conditions were different during the last deglaciation and the early to mid Holocene (e.g. Gasse et al., 1990; deMenocal et al., 2000a,b; Kuper and Kröpelin, 2006). For example, during the so-called African Humid Period (14.6–5.5 ka BP) the African monsoon system was strengthened, providing increased amounts of moisture to the study region from the Tropics in the south (deMenocal et al., 2000b; Tjallingii et al., 2008). Numerous studies document the existence of palaeoriver systems (e.g. Vörösmarty et al., 2000; Antobreh and Krastel, 2006; Zühlsdorff et al., 2007), in a region that is presently too dry for substantial fluvial runoff.

The modern hydrographic and atmospheric scenario off northwest Africa is complex (e.g. Mittelstaedt et al., 1975; Mittelstaedt, 1983, 1991; Van Camp et al., 1991). The region off Mauritania is characterised by high productivity due to strong coastal upwelling, caused by the northeastern trade winds; secondary upwelling may also occur further offshore along the shelf break (e.g. Mittelstaedt et al., 1975). Upwelling along the northwest African coast is connected with the southward flow over the shelf. Although productivity variations in coastal upwelling areas are usually attributed to changes in upwelling intensity due to wind stress (e.g. Summerhayes et al., 1995; Romero et al., 2006), the productivity dynamics off the Mauritanian coast is less straightforward owing to its complex atmospheric and hydrographic setting (Mittelstaedt, 1991; Barton, 1998). Being at the frontal zone of water masses of North and South Atlantic origin (Mittelstaedt, 1991), the primary productivity off the Mauritanian coast is strongly influenced by the nutrient content of the upwelled waters (Zenk et al., 1991). Nutrient-rich upwelled waters can have surface chlorophyll a concentrations of up to $9.0 \, mg \, m^{-3}$ (Van Camp et al., 1991) and promotes high but variable primary production year round over the shelf, and beyond the shelf break (Longhurst et al., 1995). In addition, giant filaments with chlorophyll concentrations of $1–2 \, mg \, m^{-3}$ are present in the region several hundred kilometres offshore from the shelf break (Van Camp et al., 1991).

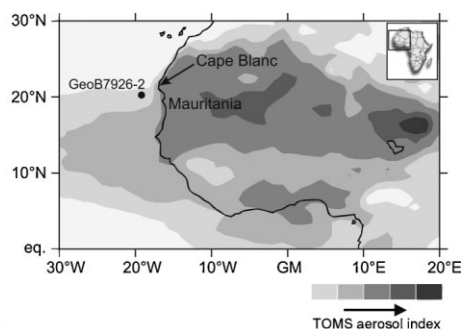The main surface current is the southward-flowing Canary Current (CC), largely connected to the atmospheric circulation along the northwest continental African margin (Mittelstaedt, 1983, 1991). Seasonal variation in the large-scale pattern of geostrophic circulation occurs, although the total transport does not vary significantly (Stramma and Siedler, 1988). In particular, the CC is stronger in summer near the African coast, while in winter it is stronger west of the Canaries (Barton, 1998). The CC separates from the African coast near Cape Blanc (21° N) and by the latitude of Cap Vert (15° N) all of the flow has turned westward to supply the North Equatorial Current (Barton, 1998). The CC is underlain by northward-flowing South Atlantic Central Water (SACW) between 200 and 600 m and the southward-flowing, deeper-running, North Atlantic Central Water (NACW) (Futterer, 1983). The less saline SACW (salinity: 35.6–35.9) constitutes a major part of the upwelled water south of Cape Blanc, whereas north of the Cape the saltier NACW (salinity: 36.1–36.4) makes up a significant portion (Mittelstaedt, 1983). Above about 300 m, the SACW mass is diverted seaward in the confluence with the CC near 21° N but, within a narrow region over the continental slope penetrates northward as an undercurrent. The SACW, modified from its original Southern Hemisphere form by mixing en route (Barton, 1998), is richer in nutrients than the NACW (Mittelstaedt, 1991, and references therein).

Material and methods

Gravity core GeoB7926-2 was retrieved during Meteor Cruise M53/1 off Mauritania, northwest Africa (20° 12.79′ N, 18° 27.14′ W, water depth 2500 m; Fig. 1). The core is 1330 cm long and this study focuses on the uppermost 500 cm, representing the last 17 ka BP. All ages are presented as calibrated ^{14}C a before present. A detailed core description was published by Meggers et al. (2003) and by Romero et al. (2008); archived core material is kept at MARUM, University of Bremen, Germany.

Chronology and accumulation rates

The age model is based on 14 accelerator mass spectrometric ^{14}C dates for the entire core on the peroxide-leached planktonic foraminifera (Globigerina inflata, >150 μm fraction), where 11 radiocarbon dates are within the core segment investigated here (Table 1; see also Romero et al., 2008). The ^{14}C dating was performed at the Leibniz Laboratory for Radiometric Dating and Stable Isotope Research (Kiel University, Germany). A reservoir age of 500 a was employed, following deMenocal et al. (2000a), and the dates were converted into calendar years BP using Calib Execute Version 5.0.2 (http://calib.qub.ac.uk/). Age estimates between dated

Figure 1. Location of site GeoB7926 (indicated by a dot) off Mauritania in the northeast Atlantic Ocean. The TOMS aerosol index is an average of aeolian particles between 1997 and 2005. (TOMS data are available at http://toms.gsfc.nasa.gov/). Figure redrawn from Mulitza et al. (2008).

Table 1. 11 AMS ^{14}C dates for gravity core GeoB7926-28.*

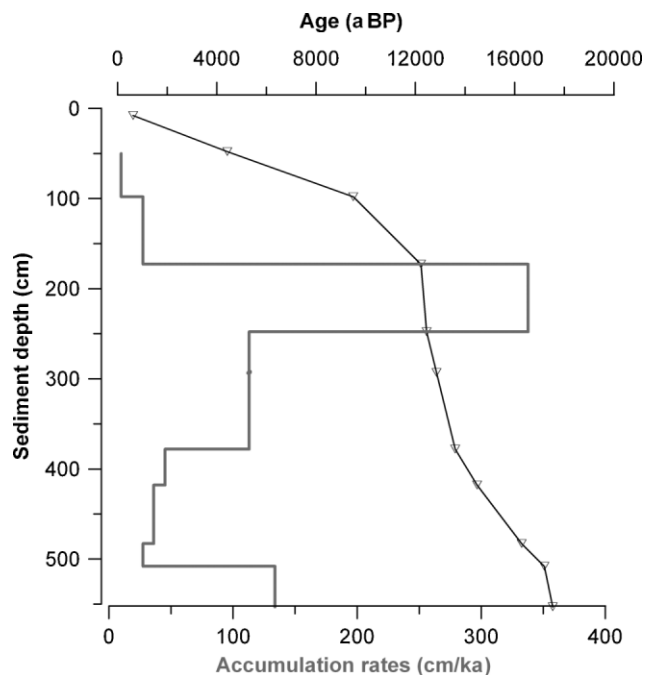| Laboratory ID No.	Interval (cm)	Age (^{14}C a BP)	± Error (a)	2σ (a BP)	Age ($\Delta R = 0$ a) (cal. a BP)
KIA 24287	8	1 170	35	50	630
KIA 25812	48	4 455	35	72	4 423
KIA 25810	98	8 970	45	30	9 495
KIA 24286	173	10 050	70	180	12 230
KIA 22417	248	10 830	70	170	12 452
KIA 24285	293	10 550	70	160	12 850
KIA 24285	378	12 220	70	100	13 602
KIA 29030	418	13 050	70	90	14 485
KIA 27310	483	14 220	100	80	16 286
KIA 29029	508	14 290	60	110	17 199
KIA 22416	553	14 670	80	140	17 535

*Analysed material was Globigerina inflata.

Figure 2. Age model (black line) based on 11 calibrated ^{14}C dates and accumulation rates (cm ka[−1], grey line) for core GeoB7926-2 (Romero et al., 2008).

levels were obtained by linear interpolation between calibrated ^{14}C dates.

The lower core section corresponds to late Heinrich event 1 (Fig. 2). The accumulation rate is ∼30 cm ka[−1] during this time and it increases to ∼35 cm ka[−1] leading up to the Bølling–Allerød. The sedimentation rate rises following a two-step pattern: the first during the Bølling–Allerød from ∼45 to 110 cm ka[−1]; the second during the Younger Dryas (up to ∼340 cm ka[−1]). The accumulation rate decreases to 28 cm ka[−1] around 12.3 ka BP, which is high for a hemipelagic setting. The abrupt decrease in the accumulation rate after the Younger Dryas might be partly an artefact. However, the radiocarbon ages show a continuous sedimentation history for the last 10 ka and no evidence of strong changes in the sedimentation pattern was observed by the visual description of GeoB7926-2 (Meggers et al., 2003) or by core logging measurements (O. E. Romero, unpublished data). This study focuses primarily on the record between approximately 17 and 4.5 ka BP.

Environmental proxies

Grain size analysis

In order to isolate the terrigenous fraction from the deep-marine sediments, several pre-treatment steps were undertaken to remove different biogenic constituents. Organic carbon (C_{org}) was removed by adding 10 mL H_2O_2 (35%) to approximately 750 mg of bulk sediment. Reaction was sped by boiling the mixture. Boiling was continued until the reaction stopped and excess H_2O_2 was decomposed into H_2O and O_2. Calcium carbonate was subsequently removed by adding 10 mL HCl (10%) to the C_{org}-free sediments in 100 mL demineralised water and boiled for 1 min. Visual checks were made to ensure the removal of all $CaCO_3$. The sample was then diluted with demineralised water until neutral pH. Biogenic silica was removed by adding 6 g NaOH pellets to the now C_{org}-free and $CaCO_3$-free sediments in 100 mL demineralised water. This mixture was boiled for 10 min and visual checks were made to ensure the removal of all diatoms and radiolarians. The solution was pH neutralised by diluting it with demineralised water. Just before the grain size analyses, the now C_{org}-free, $CaCO_3$-free

and biogenic opal-free sediments were boiled with 300 mg of the readily soluble salt sodium pyrophosphate ($Na_4P_2O_7$.$10H_2O$) to ensure disaggregation of all aggregates. Grain size distributions of the terrigenous fraction (C_{org}-free,$CaCO_3$-free and biogenic opal-free) were measured with a Coulter laser particle sizer LS200, resulting in 92 size classes from 0.4 to 1908 μm at a 5 cm (ca. 100–400 a) downcore sampling interval.

End-member modelling

In general, the terrigenous fraction of deep-sea sediments in the (sub)tropical ocean, not disturbed by post-depositional processes, can be considered a mixture of aeolian and fluvial sediments. This mixture can be unmixed into subpopulations, so-called end members that can be assigned to sediment transport mechanisms (Prins, 1999; Stuut et al., 2002; Weltje and Prins, 2003; Holz et al., 2004; Tjallingii et al., 2008); this approach is followed herein. The minimum number of end members required for a satisfactory approximation of the data is calculated from the goodness-of-fit statistics, represented by the coefficients of determination. The coefficient of determination represents the proportion of the variance of each grain size class that can be reproduced by the approximated data. This proportion is equal to the squared correlation coefficient (r^2) of the input variables and their approximated values (Weltje, 1997; Prins and Weltje, 1999). Hence the eventual outcome of the model is a statistically unique solution with end members that represent real particle size distributions. The only prescription that is used during modelling is the fact that end members may not have negative grain sizes. No predefinitions are made regarding shape, sorting or modal sizes of the end members (for more details of the application of the model to particle size distributions see Weltje and Prins, 2003).

Measurements of organic carbon

Two sample series were taken: one of 1.5 cm[3] at 1 cm resolution for diatoms, and another of ∼10 cm[3] at 5 cm intervals for total organic carbon (C_{org}) and calcium carbonate ($CaCO_3$). Average sample resolution remains below ca. 40–60 a for diatoms and decreases to ca. 100–200 a for other proxies. The sediment sample set for bulk analyses was freeze-dried and ground in an agate mortar. Total carbon contents were measured on untreated samples. After decalcification of the samples using 6 N HCl, the organic carbon content was obtained by combustion at 1050°C using a Heraeus CHN-O-Rapid elemental analyser (Müller et al., 1994).

Diatoms

The samples for diatoms analysis were prepared following the method presented by Schrader and Gersonde (1978). Qualitative and quantitative analyses were done at ×1000 magnification using a Zeiss Axioscope with phase-contrast illumination. Counts were carried out on permanent slides of acid-cleaned material (Mountex mounting medium). Several traverses across the cover-slip were examined, depending on valve abundances. At least two cover slips per sample were scanned in this way. Diatom counting of replicate slides indicates that the analytical error of the concentration estimates is ≤15%. The counting procedure and definition of counting units for diatoms to the lowest possible taxonomic level followed those of Schrader and Gersonde (1978).

Benthic foraminifera

The 10 cm[3] sediment samples for foraminiferal analysis were freeze-dried, washed over a set of sieves (63 and 150 μm) and

dried at 40°C. The fraction >150 μm was used for foraminiferal analysis and comparisons were made within the 63–150 μm fraction. Where possible >300 specimens were counted but where few specimens were present, especially in the sequences with high accumulation rates, the whole sample was counted. General information on foraminiferal analyses and preparation techniques are available in Murray (1991). Foraminiferal analyses were carried out on average at 10 cm intervals between 0 and 500 cm. Taxonomic identification follows Jones (1994), Schmiedl, (1995) and Holbourn and Henderson, (2002).

Results

Terrestrial component

The average grain size distribution of the silt fraction in core GeoB 7926 (N = 106) is bimodal, with modes around 7 and 23 μm (Fig. 3A). Figure 3B shows the coefficients of determination (r^2) plotted against grain size for models with 2–10 end members. The mean coefficient of determination of the grain size classes increases when the number of end members increases (Fig. 3B). The two-end-member model ($r^2_{mean} = 0.71$) shows low r^2 (<0.6) for the size range 9–22 μm. The three-end-member model ($r^2_{mean} = 0.86$) shows high r^2 (>0.8) for most size classes, except for the fine range (<2 μm) and between 9 and 16 μm. The four-end-member model shows high r^2 (>0.8) for the whole size spectrum except the very fine range (<0.8 μm). The goodness-of-fit statistics thus demonstrate that either the three- or four-end-member model provides the best compromise between the number of end members and r^2 (Fig. 3C). However, the shape of the size distributions of the end members of the four-end-member model is multimodal, showing that the model is trying to fit the noise in the data. Therefore, the three-end-member model forms the best choice

between satisfactory explanation of the variance in the dataset (r^2 mean 0.86) and limited number of end members.

All three resulting end members have a clearly defined dominant mode (Fig. 3D). End member EM1 has a modal grain size of ~5 μm, end member EM2 of ~30 μm and end member EM3 of ~60 μm. These absolute sizes of the end members compare very well with those of reconstructed end members found in surface sediments in the area off northwest Africa (Holz et al., 2004), as well as those in a nearby sediment core (Tjallingii et al., 2008). In addition, the grain size distributions of the wind-blown end members match closely with those from present-day dust collected at about the core site (Stuut et al., 2005, Fig. 3D). Therefore, in accordance with these studies the finest-grained end member is interpreted as fluvial mud, and the two coarser-grained as fine- and coarse aeolian dust, respectively (Fig. 3D).

The downcore proportions of the aeolian and fluvial grain size populations are plotted versus depth (Fig. 4) and can be interpreted in terms of regional climate patterns in northwest Africa during the last ca. 17 ka. The proportion of fluvial mud relative to wind-blown dust is here interpreted as a proxy for river runoff, which is ultimately linked to precipitation in the drainage area of the palaeoriver system (e.g. Stuut et al., 2002; Weltje and Prins, 2003).

The downcore records of the fluvial and aeolian sediment components show abrupt changes from dust-dominated time intervals with generally low amounts of fluvial material from 500 to 400 cm, which is equivalent to the deglaciation and Heinrich event H1, and from 320 to 150 cm, which is the time approximation to the Younger Dryas (YD). Between 420 and 320 cm – the Bølling–Allerød (B-A) – there is a persistent period of high amounts fluvial material. From 150 cm to the top of the studied core section there is a gradual increase in the amount of fluvial material, and the aeolian material in this interval is
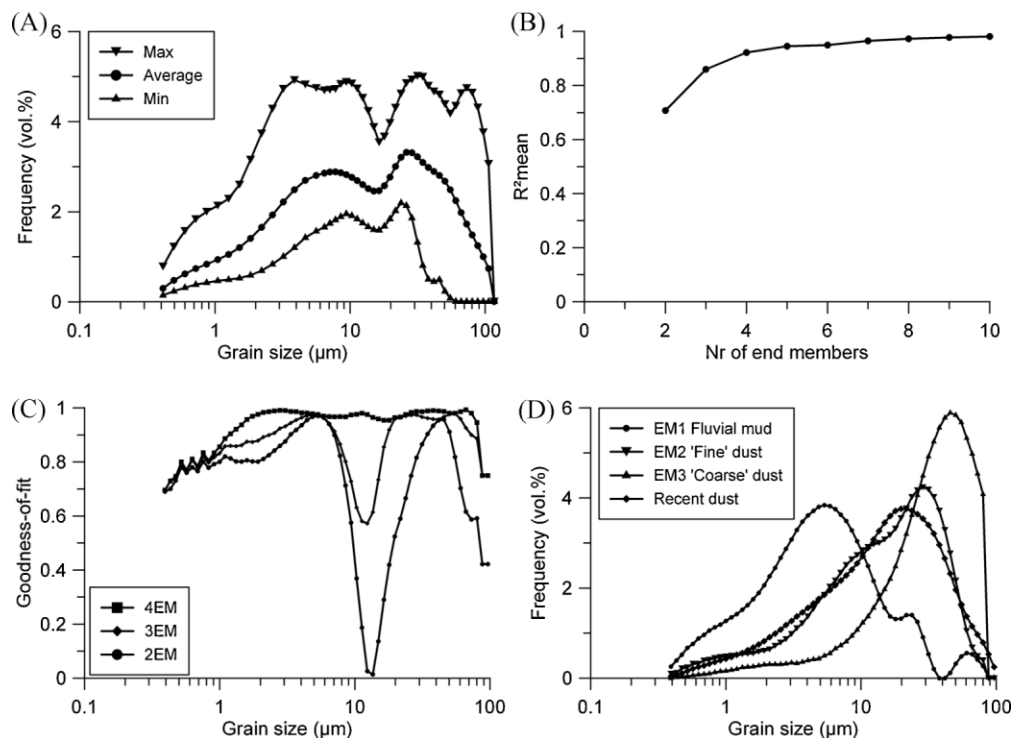

Figure 3. Particle size and end-member modelling results for core GeoB 7926-2. (A) Data statistics (average grain size distribution, maximum and minimum envelope) of the whole particle size dataset (N = 106); (B) mean coefficient of determination (r^2_{mean}) of all size classes for each end-member model; (C) r^2 (goodness-of-fit) of models with two to four end members for each particle size class; (D) comparison of particle size distributions for the end members from the three-end-member model with present-day dust collected near to site GeoB7926-2 (Stuut et al., 2005).
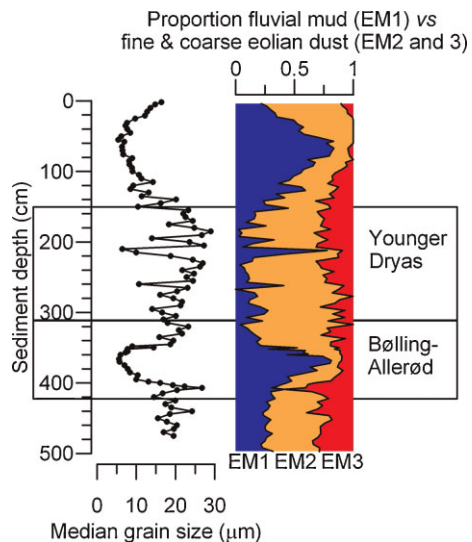
Figure 4. The result of the grain size analysis: medium grain size data and the relative proportions of end members (EM)1–3, where EM1 indicates the fluvial component, EM2 and EM3 fine and coarse aeolian dust, respectively.
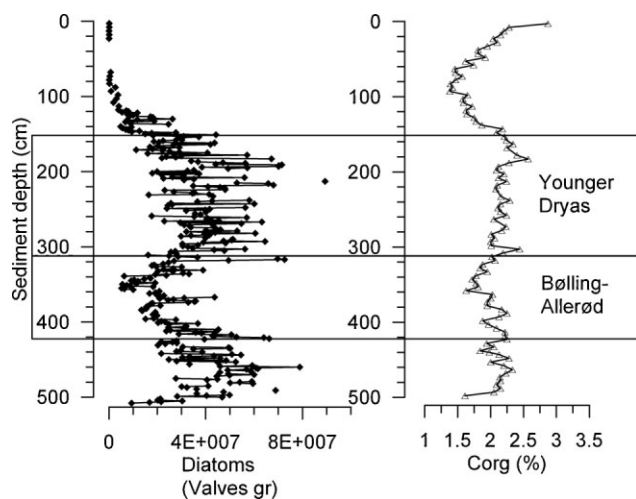

Figure 5. The abundance of diatoms (valves g^{-1}) together with organic carbon content for core GeoB 7926-2 presented *versus* sediment depth (cm).

typified by gradually decreasing proportions of coarse dust (Fig. 4).

Sea surface and sea floor environment

The diatom abundance reaches extremely high values during the late H1 and the YD (up to 8×10^7 valves g^{-1}; Fig. 5), whereas it decreases to an average of 2×10^7 valves g^{-1} during the B-A. The highly diversified diatom assemblage, consisting of almost 200 species, is dominated by the resting spores of *Chaetoceros* species throughout the deglaciation (Romero *et al.*, 2008).

The organic carbon content (C_{org}) varies between 1.4% and 2.6%, with an average of 2.0% over the studied core section (Fig. 5). The C_{org} content decreases during the B-A compared to late H1, and varies between 1.6% and 2.3% (Fig. 5). The YD is characterised by the highest organic carbon content, on average 2.2%. The C_{org} content decreases notably following the YD.

The benthic foraminiferal fauna consists of low-abundant, typical deep-sea species. More than 115 species were identified but only the most common ones, with relative abundances

above 3% and occurrences during the B-A and YD, are discussed here. The number of species and the abundances increase from 24 to 32 species on average and from 32 to 45 specimens cm^{-3} at the onset of the B-A (Fig. 6). The prominent species during the B-A period are *Bulimina exilis* (34%), *Nonionella iridea* (8%), *Planulina wuellerstorfi* (7%), *Melonis barleeanum* (5%), *Melonis pompiliodes* (5%), *Cassidulina laevigata* (4%) *Pyrgo* sp. (4%), *Globobulima turgida* (3%) and *Quinqueloculina seminulum* (3%), in order of occurrence, where the percentage values represent averages (Fig. 6). Also different species of *Uvigerina*, such as *U. auberiana*, *U. hispida*, *U. mediterranea*, *U. peregrina* and *U. proboscidea*, form an important component of the fauna, together representing on average 5%. The faunal composition changes markedly at the onset of the YD; the number of species decreases to 16 on average and the abundance reduces to 14 specimens cm^{-3} (Fig. 6). However, the foraminiferal flux does not change as distinctly; instead it fluctuates during the YD. The most striking feature is the marked change in species composition, with several species disappearing during this time interval. The dominating species during the YD are *B. exilis* (66%), *N. iridea* (6%), *Nonionella turgida* (4%), *G. turgida* (4%) and *Chilostomella ovoidea* (3%) (Fig. 6). During one brief period around 12.4 ka BP the species more characteristic for the B-A period return briefly to the region but disappear again within less than 100 a; *B. exilis* continues to dominate the fauna. After the YD, the foraminiferal fauna changes again; the species common during the B-A return to the region and dominate the faunal composition throughout the Holocene. *Bulimina exilis* disappears around 10 ka BP.

Discussion

The links between climate variability in continental northwest Africa and in the adjacent ocean are detailed here. Strong biogenic responses to environmental changes both in the upper part of the water column and on the sea bottom are observed. In particular, the potential relationship between the terrigenous input, surface-ocean productivity and the deep-sea benthic communities in the Mauritanian upwelling region are investigated. On combining several proxies, a general pattern of variability is recognised: changes in the intensity of trade-wind-induced upwelling lead to changes in the primary productivity in the surface ocean, which is potentially also fertilised by nutrients carried by the deposited aeolian dust. As a result of the increased diatom and organic matter fluxes to the sea floor, the dissolved oxygen content at the sea floor decreased radically, with major consequences for benthic life during part of the deglaciation (Fig. 7).

Between ca. 17 and 15 ka BP there is a rather constant contribution of the different sediment components in core GeoB7926-2 (Figs 4 and 7). During the B-A, however, there is a dominance of the fluvial component of the terrigenous input at the site and this is interpreted in terms of more humid conditions on the continent (Figs 4 and 7). The humid conditions during the B-A along the western African coast agree well with the reconstructed scenarios presented by recent studies (e.g. Mulitza *et al.*, 2008; Romero *et al.*, 2008; Tjallingii *et al.*, 2008). Several authors now regard the onset of the African Humid Period to be roughly coincident with the B-A period (deMenocal *et al.*, 2000b; Gasse, 2000; Adkins *et al.*, 2006).

The total diatom concentration decreased during the B-A, probably as a consequence of weakened upwelling and decreased dust input combined with silica-depleted upwelled waters off Mauritania, delivered by the NACW (Romero *et al.*, 2008). The rapidity and magnitude of the B-A warming resulted
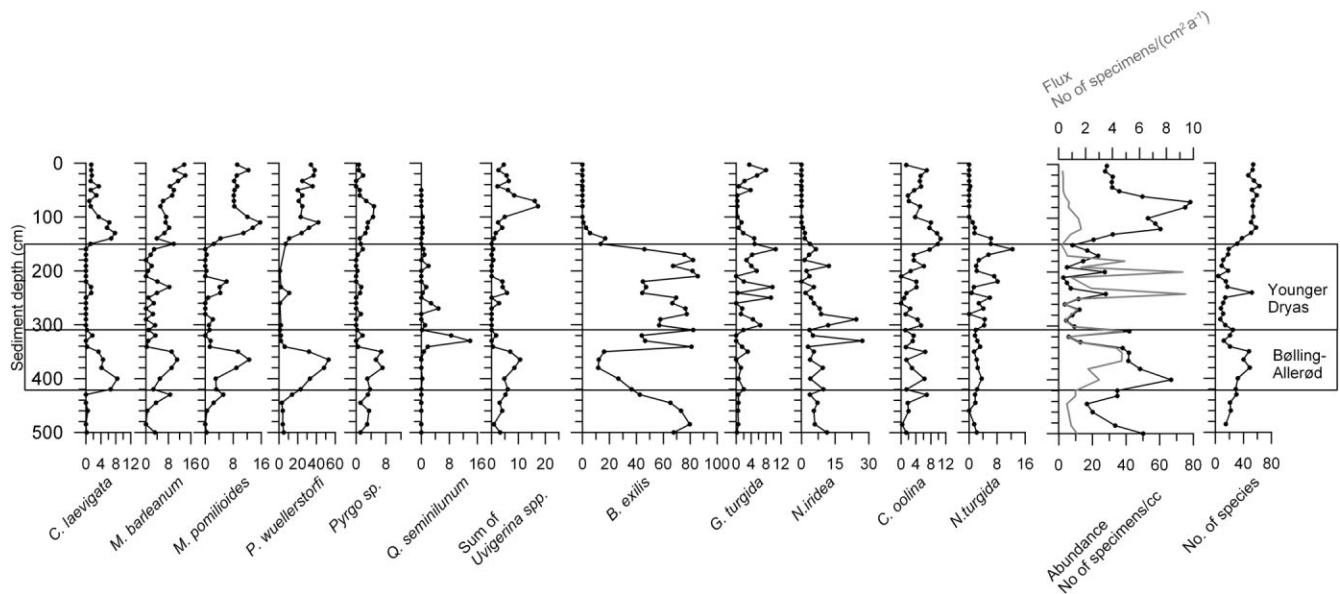
Figure 6.   The relative abundances of the most common benthic foraminiferal species in core GeoB 7926-2 together with flux (number of specimens per cm² and year, grey line), total number of specimens per cubic centimetre (black line) and number of species.

in large part from the reinvigoration of the Atlantic meridional overturning circulation (MOC) (McManus *et al.*, 2004). This might, in turn, have strengthened the southward intrusion of silica-depleted NACW and thus caused an abrupt decrease in diatom production off Mauritania (Romero *et al.*, 2008).

The benthic foraminiferal fauna during the B-A indicates environmental conditions similar to those of today, with the exception of the occurrence of *B. exilis*, which is a rather uncommon species in bottom sediments of late Holocene age off Mauritania (Morigi *et al.*, 2001). The high relative contribution of *B. exilis*, together with a high benthic foraminifera species diversity, suggest an organic matter-enriched, well-oxygenated sea-bottom environment; this is further supported by the relatively high C_{org} content (Fig. 7).

The relatively humid conditions that prevailed during the B-A are followed by an abrupt shift in the contribution of fluvial material at the onset of YD, and the wind-blown sediment proportion contains a considerable amount of coarse aeolian dust (Figs 4 and 7). This represents the relatively dry and windy conditions on the northwest African continent during the YD.

Several studies document drier conditions in northern Africa during the YD as compared to B-A (e.g. Street-Perrott and Perrott, 1990; deMenocal *et al.*, 2000b; Lancaster *et al.*, 2002; Mulitza *et al.*, 2008; Romero *et al.*, 2008; Tjallingii *et al.*, 2008), probably due to more intense northeastern trade winds. A number of palaeoclimatological and modelling studies (e.g. deMenocal and Rind, 1993; Marret and Turon, 1994; Lezine and Denefle, 1997; Lancaster *et al.*, 2002; Dahl *et al.*, 2005; Mulitza *et al.*, 2008) have demonstrated increased northeastern trade winds over northwest Africa during the YD as a response to lower sea surface temperatures. In addition, the slowdown of the MOC during the YD (McManus *et al.*, 2004) most likely favoured siliceous productivity off Mauritania due to increased supply of Si by SACW (Romero *et al.*, 2008). The diatom productivity reached exceptionally high values (up to 8×10^7 valves g^{-1}) during the YD (Fig. 5). As a result of the enhanced lithogenic input and the high surface water productivity, high sedimentation and accumulation rates occurred at the site during the YD (Fig. 3). Although atmospheric conditions off Mauritania during the YD resembled those of H1 (Romero *et al.*,
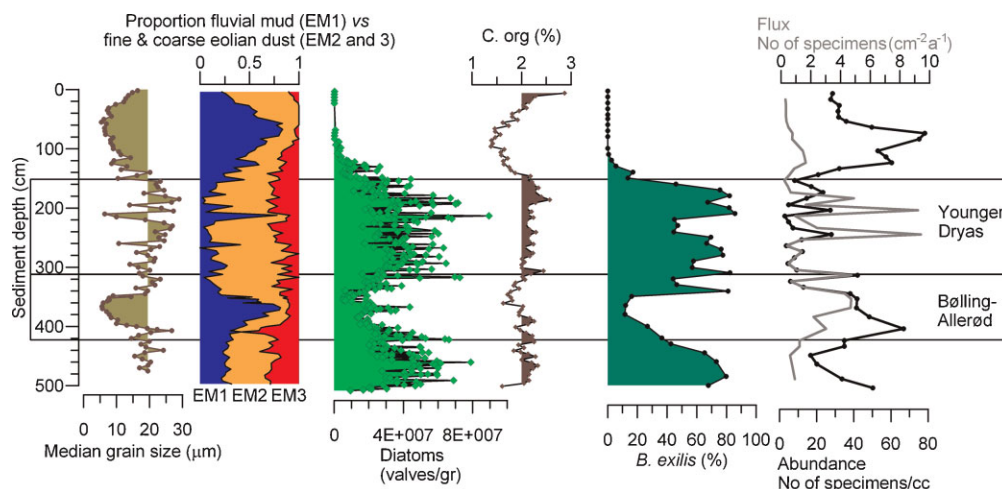

Figure 7.   Summary figure of analysed proxy data. The two left panels indicate grain size data: medium grain size data and the relative proportions of end members (EM)1–3, where EM1 indicates the fluvial component, and EM2 and EM3 fine and coarse aeolian dust, respectively. The two middle panels show the organic carbon content and the abundance of diatoms (valves g^{-1}). The two far right panels demonstrate the benthic component; the relative abundance of the low-oxygen-tolerant benthic foraminifera *B. exilis* and the flux (number of specimens per cm² and year) and the total number of benthic foraminifera per cubic centimetre.

2008), the enhanced wind intensity and the high sedimentation rates suggest that wind played a crucial role in determining upwelling intensity and seaward Ekman transport. Favourable conditions for diatom productivity in surface waters prevailed throughout the YD, although weak incursions of open ocean waters into the coastal area of Cape Blanc are reflected by the occurrence of diatoms typical of pelagic, oligotrophic waters (Romero et al., 2002, 2008).

At the onset of YD, the deep-sea foraminiferal fauna that had been dominated by B. exilis, C. laevigata, G. turgida, M. barleeanum, M. pompiliodes, N. iridea, P. wuellerstorfi, Pyrgo sp., Q. seminulum and several Uvigerina species changed its composition to a large extent with respect to both diversity and abundance. The fauna during YD became dominated almost entirely by the thin-shelled and small-sized B. exilis (Figs 6 and 7). Bulimina exilis is known to be abundant during times of high diatom production (Caralp, 1989) and since the sediments at site GeoB7926 received a large input of diatoms both during the B-A and the YD it is not surprising that B. exilis is one of the dominating species. However, the question is how the benthic environment changed during the onset of the YD; considerable environmental changes must have occurred as the foraminiferal fauna changes were so substantial. Deep-sea benthic foraminifera distributions are, in general, controlled by the dissolved oxygen concentrations of bottom and pore waters, and by the input of organic matter (e.g. Loubere and Fariduddin, 1999; Murray 2001; Jorissen et al., 2007). The supply of labile organic matter, through diatom input, increased considerably during the YD. This would potentially benefit the benthic foraminiferal fauna, especially species like M. barleeanum, M. pomilioides and Uvigerina spp., which are known to proliferate in organic-enriched environments (e.g. Zarriess and Mackensen, 2010, and references therein). However, the opposite occurred: the aforementioned species became very low in abundance and therefore some other environmental factors, together with the input of organic matter, must have contributed to the faunal dominance of B. exilis. As stated above, the bottom-water dissolved oxygen concentration of the bottom water is one of the two major controlling factors and it is very likely that the high input of organic matter, delivered by the exceptionally high concentrations of diatoms, caused low-oxygen conditions at site GeoB7926 during the YD. A close link between low-oxygen conditions and high abundance of B. exilis has also been documented for several high-productivity areas such as the Arabian Sea (Jannink et al., 1998) and the Benguela upwelling system (Brüchert et al., 2000); our record is the first for northwest Africa during the YD. The dominance of the benthic foraminifer B. exilis also suggests that conditions in the benthic environment off Mauritania during the YD differed from the present-day upwelling conditions, since low-oxygen conditions are unknown during modern times (Lutze and Coulbourn, 1984); nor is B. exilis a common species (Lutze and Coulbourn, 1984; Morigi et al., 2001). This interpretation is further supported by modern moderate to low fluxes of diatoms off Cape Blanc (Romero et al., 2002). The combination of high organic matter deposition due to the very high surface water productivity and the subsequent low-oxygen conditions is the most likely explanation for the benthic faunal response.

Conclusions

This study demonstrates that humid conditions prevailed in the Mauritania region during the Bølling–Allerød, with a large fluvial lithogenic input delivered into the Mauritanian upwelling area. Climate conditions on the northwest African continent became drier during the Younger Dryas and, probably as a result of increased trade-wind-driven upwelling, surface primary productivity off Cape Blanc increased. The very high input of labile organic matter caused low-oxygen conditions at the sea floor, here illustrated by the dominance of the benthic foraminifera Bulimina exilis and a poorly diversified benthic foraminiferal fauna. The occurrence of low-oxygen conditions in this upwelling region during the Younger Dryas has previously been unknown; however, more detailed knowledge is warranted to identify the spatial extension of the low-oxygen conditions and to fully understand the relationships between changes in upwelling intensity, productivity and response of the benthic ecosystem.

Abbreviations. B-A, Bölling-Alleröd; CC, Canary Current; C_{org}, organic carbon; H1, Heinrich event H1; MOC, meridional overturning circulation; NACW, North Atlantic Central Water; SACW, South Atlantic Central Water; YD, Younger Dryas.

References

Adkins J, deMenocal PB, Eshel G. 2006. The 'African humid period' and the record of marine upwelling from excess Th-230 in Ocean Drilling Program Hole 658C. Paleoceanography 21: 4203.

Antobreh AA, Krastel S. 2006. Morphology, seismic characteristics and development of Cap Timiris Canyon, offshore Mauritania: a newly discovered canyon preserved-off a major arid climatic region. Marine and Petroleum Geology 23: 37–59.

Barton ED. 1998. Eastern boundary of the North Atlantic: northwest Africa and Iberia. In The Sea, Vol. 11, Robinson AR, Brink KH (eds). John Wiley and Sons: New York; pp. 633–657.

Brüchert V, Perez ME, Lange CB. 2000. Coupled primary production, benthic foraminiferal assemblage, and sulfur diagenesis in organic-rich sediments of the Benguela upwelling system. Marine Geology 163: 27–40.

Caralp MH. 1989. Abundance of Bulimina exilis and Melonis barleeanum: relationship to the quality of marine organic matter. Geo-Marine Letters 9: 37–43.

Castaneda IS, Mulitza S, Schefuss E, et al. 2009. Wet phases in the Sahara/Sahel region and human migration patterns in North Africa. Proceedings of the National Academy of Sciences of the USA 106: 20159–20163.

Dahl K, Broccoli A, Stouffer R. 2005. Assessing the role of North Atlantic freshwater forcing in millennial scale climate variability: a tropical Atlantic perspective. Climate Dynamics 24: 325–346.

deMenocal PB, Rind D. 1993. Sensitivity of Asian and African climate to variation in seasonal insolation, glacial ice cover, sea-surface temperature, and Asian orography. Journal of Geophysical Research: Atmospheres 98: 7265–7287.

deMenocal PB, Ortiz J, Guilderson T, et al. 2000a. Coherent high- and low-latitude climate variability during the Holocene Warm Period. Science 288: 2198–2202.

deMenocal PB, Ortiz J, Guilderson TP, et al. 2000b. Abrupt onset and termination of the African Humid Period: rapid climate responses to gradual insolation forcing. Quaternary Science Reviews 19: 347–361.

Futterer DK. 1983. The modern upwelling record off Northwest Africa. In Coastal Upwelling: Its Sediment Record, Part B. Sedimentary Records of Ancient Coastal Upwelling, Thiede J, Suess E (eds). Plenum Press: London; 105–121.

Garcin Y, Vincens A, Williamson D, *et al.* 2007. Abrupt resumption of the African Monsoon at the Younger Dryas–Holocene climatic transition. *Quaternary Science Review* **26**: 690–704.

Gasse F. 2000. Hydrological changes in the African tropics since the Last Glacial Maximum. *Quaternary Science Reviews* **19**: 189–211.

Gasse F, Tehet R, Durand A, *et al.* 1990. The arid–humid transition in the Sahara and the Sahel during the last deglaciation. *Nature* **346**: 141–146.

Herguera JC, Berger WH. 1991. Paleoproductivity from benthic foraminifera abundance: glacial to postglacial change in the west-equatorial Pacific. *Geology* **19**: 1173–1176.

Holbourn AE, Henderson AS. 2002. Re-illustration and revised taxonomy for selected deep-sea benthic foraminifers. *Paleontologia Electronica* **4**: 34 pp. [http://palaeo-electronica.org/paleo/2001/foram/issue2_01.htm]

Holz C, Stuut J-BW, Henrich R. 2004. Terrigenous sedimentation processes along the continental margin off NW-Africa: implications from grain-size analyses of surface sediments. *Sedimentology* **51**: 1145–1154.

Jannink NT, Zachariasse WJ, Van der Zwaan GJ. 1998. Living (Rose Bengal stained) benthic foraminifera from the Pakistan continental margin (northern Arabian Sea). *Deep-Sea Research Part I: Oceanographic Research Papers* **45**: 1483–1513.

Jones RW. 1994. *The Challenger Foraminifera*. Natural History Museum/Oxford University Press: London.

Jorissen F, Fontainer C, Thomas E. 2007. Paleoceanographic proxies based on deep-sea benthic foraminiferal assemblage characteristics. In *Proxies in Late Cenozoic Paleoceanography*, Hillaire-Marcel C, de Vernal A (eds). Developments in Marine Geology. Elsevier: Amsterdam; 263–326.

Kim JH, Meggers H, Rimbu N, *et al.* 2007. Impacts of the North Atlantic gyre circulation on Holocene climate off northwest Africa. *Geology* **35**: 387–390.

Kröpelin S, Verschuren D, Lézine A-M, *et al.* 2008. Climate-driven ecosystem succession in the Sahara: the past 6000 years. *Science* **320**: 752–753.

Kuhlmann H, Meggers H, Freudenthal T, *et al.* 2004. The transition of the monsoonal and the N Atlantic climate system off NW Africa during the Holocene. *Geophysical Research Letters* **31**: L22204.

Kuper R, Kröpelin S. 2006. Climate-controlled Holocene occupation in the Sahara: motor of Africa's evolution. *Science* **313**: 803–807.

Lancaster N, Kocurek G, Singhvi A, *et al.* 2002. Late Pleistocene and Holocene dune activity and wind regimes in the western Sahara Desert of Mauritania. *Geology* **30**: 991–994.

Lezine AM, Denefle M. 1997. Enhanced anticyclonic circulation in the eastern North Atlantic during cold intervals of the last deglaciation inferred from deep-sea pollen records. *Geology* **25**: 119–122.

Longhurst AL, Sathyendranath S, Platt T, *et al.* 1995. An estimate of global primary production from satellite radiometer data. *Journal of Plankton Research* **17**: 1245–1271.

Loubere P. 1991. Deep-sea benthic foraminiferal assemblage response to a surface ocean productivity gradient: a test. *Paleoceanography* **6**: 193–204.

Loubere P, Fariduddin M. 1999. Benthic Foraminifera and the flux of organic carbon to the seabed. In *Modern Foraminifera*, Sen Gupta BK (ed.). Kluwer Academic: Dordrecht; 181–200.

Lutze GF, Coulbourn WT. 1984. Recent benthic foraminifera from the continental margin of northwest Africa: community structure and distribution. *Marine Micropaleontology* **8**: 361–401.

Marret F, Turon JL. 1994. Paleohydrology and paleoclimatology off northwest Africa during the last glacial interglacial transition and the Holocene: palynological evidences. *Marine Geology* **118**: 107–117.

McGregor HV, Dima M, Fischer HW, *et al.* 2007. Rapid 20th-century increase in coastal upwelling off northwest Africa. *Science* **315**: 637–639.

McManus JF, Francois R, Gherardi JM, *et al.* 2004. Collapse and rapid resumption of Atlantic meridional circulation linked to deglacial climate changes. *Nature* **428**: 834–837.

Meggers H, Babero-Munoz L, Barrera C, *et al.* 2003. Report and preliminary results of METEOR cruise M 53/1, Limassol–Las Palmas–Mindelo, 30.03.–03.05.2002. *Berichte aus dem Fachbereich Geowissenschaften der Universität Bremen*. Universität Bremen.

Mittelstaedt E. 1983. The upwelling area off northwest Africa: a description of phenomena related to coastal upwelling. *Progress in Oceanography* **12**: 307–331.

Mittelstaedt E. 1991. The ocean boundary along the northwest African coast: circulation and oceanographic properties at the sea surface. *Progress in Oceanography* **26**: 307–355.

Mittelstaedt E, Pillsbury D, Smith RL. 1975. Flow patterns in the northwest African upwelling area. *Deutsche Hydrographische Zeitschrift* **28**: 145–167.

Morigi C, Jorissen FJ, Gervais A, *et al.* 2001. Benthic foraminiferal faunas in surface sediments off NW Africa: relationship with organic flux to the ocean floor. *Journal of Foraminiferal Research* **31**: 350–368.

Mulitza S, Prange M, Stuut J-BW, *et al.* 2008. Sahel megadroughts triggered by glacial slowdowns of Atlantic meridional overturning. *Paleoceanography* **23**: PA4206.

Mulitza S, Heslop D, Pittauerova D, *et al.* 2010. Increase in African dust flux at the onset of commercial agriculture in the Sahel region. *Nature* **466**: 226–228.

Müller P, Schneider RR, Ruhland G. 1994. Late Quaternary pCO$_2$ variations in the Angola Current: evidence from organic carbon δ^{13}C and alkenone temperatures. In *Carbon Cycling in the Glacial Ocean: Constraints on the Ocean's Role in Global Change*, Vol. 17, Zahn R, Pedersen TF, Kaminski MA. Labeyrie L (eds). Springer: Heidelberg; 343–366.

Murray JW. 1991. *Ecology and Palaeoecology of Benthic Foraminifera*. Longman Scientific and Technical: Harlow, UK.

Murray JW. 2001. The niche of benthic foraminifera, critical thresholds and proxies. *Marine Micropaleontology* **41**: 1–7.

Nelson DM, Tréguer P, Brzezinski MA, *et al.* 1995. Production and dissolution of biogenic silica in the ocean: revised global estimates, comparison with regional data and relationship to biogenic sedimentation. *Global Biogeochemical Cycles* **9**: 359–372.

Prins MA. 1999. *Pelagic, hemipelagic and turbidite deposition in the Arabian Sea during the Late Quaternary*. PhD thesis, Utrecht University.

Prins MA, Weltje GJ. 1999. End-member modeling of siliciclastic grain-size distributions: the Late Quaternary record of eolian and fluvial sediment supply to the Arabian Sea and its paleoclimatic significance. In *Numerical Experiments in Stratigraphy: Recent Advances in Stratigraphic and Sedimentologic Computer Simulations*, Harbaugh J, Watney L, Rankey G, Slingerl R, Goldstein R, Franseen E (eds). Special Publication 62. SEPM: Tulsa, OK: 91–111.

Ragueneau O, Tréguer P, Leynart A, *et al.* 2000. A review of the Si cycle in the modern ocean: recent progress and missing gaps in the application of biogenic opal as a paleoproductivity proxy. *Global Planetary Change* **26**: 317–365.

Romero OE, Lange CB, Wefer G. 2002. Interannual variability (1988–1991) of siliceous phytoplankton fluxes off northwest Africa. *Journal of Plankton Research* **24**: 1035–1046.

Romero OE, Kim J-H, Hebbeln D. 2006. Paleoproductivity evolution off central Chile from the Last Glacial Maximum to the Early Holocene. *Quaternary Research* **65**: 519–525.

Romero OE, Kim JH, Donner B. 2008. Submillennial-to-millennial variability of diatom production off Mauritania, NW Africa, during the last glacial cycle. *Paleoceanography* **23**: PA3218.

Schmiedl G. 1995. *Late Quaternary benthic foraminiferal assemblages from the eastern South Atlantic Ocean: reconstruction of deep water circulation and productivity changes*. PhD thesis, Berichte zur Polarforschung, Alfred Wegener Institute for Polar and Marine Research, Bremerhaven.

Schrader H-J, Gersonde R. 1978. Diatoms and silicoflagellates. In *Micropaleontological counting methods and techniques: an exercise on an eight meter section of the Lower Pliocene of Capo Rosello, Sicily*, Zachariasse WJ, Riedel WR, Sanfilippo A, Schmidt, RR, Brolsma MJ, Schrader H, Gersonde R, *et al.* (eds). *Utrecht Micropaleontological Bulletin* **17**: 129–176.

Stramma L, Siedler G. 1988. Seasonal changes in the North Atlantic Subtropical Gyre. *Journal of Geophysical Research* **93**: 8111–8118.

Street-Perrott FA, Perrott RA. 1990. Abrupt climate fluctuations in the Tropics: the influence of Atlantic ocean circulation. *Nature* **343**: 607–612.

Stuut J-BW, Prins MA, Schneider RR, *et al*. 2002. A 300-kyr record of aridity and wind strength in southwestern Africa: inferences from grain-size distributions of sediments on Walvis Ridge, SE Atlantic. *Marine Geology* **180**: 221–233.

Stuut J-BW, Zabel M, Ratmeyer V, *et al*. 2005. Provenance of present-day eolian dust collected off NW Africa. *Journal of Geophysical Research* **110**: D04202.

Summerhayes CP, Kroon D, Rosell-Mellé A, *et al*. 1995. Variability in the Benguela Current upwelling system over the past 70,000 years. *Progress in Oceanography* **35**: 207–251.

Talbot MR, Filippi ML, Bo Jensen N, *et al*. 2007. An abrupt change in the African monsoon at the end of the Younger Dryas. *Geochemistry, Geophysics, Geosystems* **8**: 1–16.

Thomas E, Booth L, Maslin M, *et al*. 1995. Northeastern Atlantic benthic foraminifera during the last 45,000 years: changes in productivity seen from the bottom up. *Paleoceanography* **10**: 545–562.

Tjallingii R, Claussen M, Stuut J-BW, *et al*. 2008. Coherent high- and low-latitude control of the northwest African hydrological balance. *Nature Geoscience* **1**: 670–675.

Tréguer P, Nelson DM, Van Bennekom AJ, *et al*. 1995. The silica balance in the world ocean: a reestimate. *Science* **268**: 375–379.

Van Camp L, Nykjaer L, Mittelstaedt E, *et al*. 1991. Upwelling and boundary circulation off northwest Africa as depicted by infrared and visible satellite observations. *Progress in Oceanography* **26**: 357–402.

Vörösmarty CJ, Fekete BM, Meybeck M, *et al*. 2000. Global system of rivers: its role in organizing continental land mass and defining land-to-ocean linkages. *Global Biogeochemical Cycles* **14**: 599–621.

Weltje G. 1997. End-member modelling of compositional data: numerical–statistical algorithms for solving the explicit mixing problem. *Journal of Mathematical Geology* **29**: 503–549.

Weltje GJ, Prins MA. 2003. Muddled or mixed? Inferring palaeoclimate from size distributions of deep-sea clastics. *Sedimentary Geology* **162**: 39–62.

Zarriess M, Mackensen A. 2010. The tropical rainbelt and productivity changes off northwest Africa: a 31,000-year high-resolution record. *Marine Micropaleontology* **76**: 76–91.

Zenk W, Klein B, Schröder M. 1991. Cape Verde Frontal Zone. *Deep-Sea Research* **38**: S505–S530.

Zühlsdorff C, Wien K, Stuut J-BW, *et al*. 2007. Late Quaternary sedimentation within a submarine channel-levee system offshore Cap Timiris, Mauritania. *Marine Geology* **240**: 217–234.